www.czasopisma.pan.pl PAN POLSKA AKADEMIA NAUK www.journals.pan.pl

PAN ARCHIVES OF ACOUSTICS
Vol. **45**, No. 1, pp. 119–127 (2020)
DOI: 10.24425/aoa.2020.132488

Research Paper

Influence of Double-Panel Structure Modification on Vibroacoustical Properties of a Rigid Device Casing

Anna CHRAPOŃSKA*, Jarosław RZEPECKI, Krzysztof MAZUR
Stanisław WRONA, Marek PAWEŁCZYK

Silesian University of Technology
Institute of Automatic Control
Akademicka 16, 44-100 Gliwice, Poland
e-mail: {jaroslaw.rzepecki, krzysztof.jan.mazur, stanislaw.wrona, marek.pawelczyk}@polsl.pl
*Corresponding Author e-mail: anna.chraponska@polsl.pl

(*received April 1, 2019; accepted October 9, 2019*)

Nowadays, noise generated by devices is a serious issue in industry and in everyday life, because it may cause health damage to humans. In this research, a cubic rigid device casing built of double-panel thin steel walls is employed to reduce noise emitted from an enclosed noise source. Double-panel structure is used because of good sound insulation it provides. There exist three main groups of noise reduction methods, i.e. passive, semi-active and active. In this paper, a semi-active modification of double-panel structure is applied and examined. The bistable actuator (solenoid) mounted between incident and radiating plates changes its state due to applied constant voltage, causing the coupling of plates. Experimentally measured natural frequencies and modeshapes of the structure are compared to the simulation results. The influence of proposed modification on dynamical properties of the structure is analyzed and discussed.

Keywords: noise control; vibration control; double-panel structures; active casing; natural frequencies; modeshapes.

1. Introduction

People are exposed to health-damaging noise generated mainly by industrial machines and electric appliances. It is desirable to reduce noise in a human environment, as it also influences mental performance, and causes behavioral disturbances (Alimohammadi, Ebrahimi, 2017). In many systems, it is also important to reduce selected vibration frequencies, as they may have an impact on human body systems, for instance in the suspension of the seat (Sibielak *et al.*, 2015).

To reduce noise in the environment, several methods may be applied. The noise and vibration reduction methods may be classified into three groups: active, semi-active and passive. Noise reduction achieved using passive barriers is mainly effective at high frequencies. At the low-frequency range, their mass, cost, dimensions and thickness increase. Then, active or semi-active methods may be rather employed. The active methods are a light-weight solution for low-frequency noise and vibration problems (Elliott, 2001). The semi-active methods, however less efficient than the active solutions, may provide several benefits, such as little demand for external energy sources (Rzepecki *et al.*, 2019).

For noise and vibration reduction, single-panel structures are usually employed. Nowadays, active vibration control of thin wall casings built of modern materials has been developed, as an efficient alternative for passive solutions (Leniowska, Sierzęga, 2019). Double panels have also attracted attention because of good sound insulation they provide (Mao, Pietrzko, 2013). However, their acoustic performance deteriorates at low frequency, around the mass-air-mass resonance (Pietrzko, Mao, 2008). Many researchers employ active methods to control sound transmission through double walls (Bao, Pan, 1997; Ma *et al.*, 2016; Morzyński, Szczepański, 2018; Wrona, Pawełczyk, 2018), however there are also many studies dedicated to passive solutions (Oliazadeh *et al.*, 2019; Kim *et al.*, 2016).

For noise reduction, device casings enclosing noise sources may be utilized in each of three approaches –

active, semi-active or passive. Many studies are dedicated to specially designed casings employed, e.g. for active structural acoustic control (Chrapońska *et al.*, 2019). In this research, a rigid device casing with double-panel walls is employed to reduce noise. A modification of double-panel structure is applied with a solenoid, and examined. The modification is considered as semi-active, because the energy source is used only to supply the actuator (solenoid) and change the properties of the structure. Any control of the actuator is not employed. The presented research aims to examine an influence of such novel modification on vibroacoustical properties of casing walls.

The remainder of the paper is organized in four sections. Section 2 describes the laboratory setup with the rigid device casing. The double-panel structure modification employed in the casing is presented, and the experiment assumptions are provided. Section 3 provides theory of free vibrations of an isotropic square panel with fully clamped boundary conditions. Simulation results are presented and discussed. Section 4 provides analysis of experimentally measured natural frequencies and modeshapes. The experiment results are compared to simulation output. In Sec. 5, summary is provided, and the conclusions are drawn.

2. Setup and experiments

2.1. The laboratory setup

The examined rigid device casing is presented in Fig. 1. Front, back, left and right casing walls are built of double panels (except a single-panel top wall and sound-insulated basis). The distance between panels in a double wall equals 50 mm. Each panel is a steel square panel (0.46×0.46 m) of thickness equal to h = 0.6 mm.

Fig. 1. Front wall of the rigid device casing.

Panels are attached to a rigid frame made of 3 mm thick welded steel profiles by 20 screws (Wrona, Pawełczyk, 2018) and additionally clamped to the structure using a square frame. Hence, panels dimensions considered in vibration analysis are 0.42×0.42 m. Inside the casing, an active Behringer speaker is placed as an enclosed noise source, with its cone located in front of the examined (front) casing wall, at the distance of 10 cm.

One of double-panel casing walls was modified to provide a possibility of panels coupling. Details of the modification are described in Subsec. 2.2. The inner panel is referred to as the incident panel and the outer panel is referred to as the radiating panel (Mao, Pietrzak, 2013). To measure panel vibrations, a 7×7 grid consisting of 49 points was marked on the radiating panel of the rigid device casing. Vibrations were measured using laser vibrometer Polytec PDV-100. In the cavity between panels of left, right and back walls, a sound-absorbing foam was placed.

National Instruments PCI-6289 M Series DAQ card was used to generate multi-sinusoidal signal (up to 500 Hz, emitted from the active speaker placed inside the casing), as an excitation, and to acquire data from the laser vibrometer. Software for measurement system, designed to acquire raw measurement data and save them in files, was created in LabVIEW graphical environment. Further data processing (to compute natural frequencies and obtain modeshapes) and modeling was provided using open source software: Octave and FreeFem++ (open source partial differential equation solver which uses the Finite Element Method). The experimental setup is presented in Fig. 2.

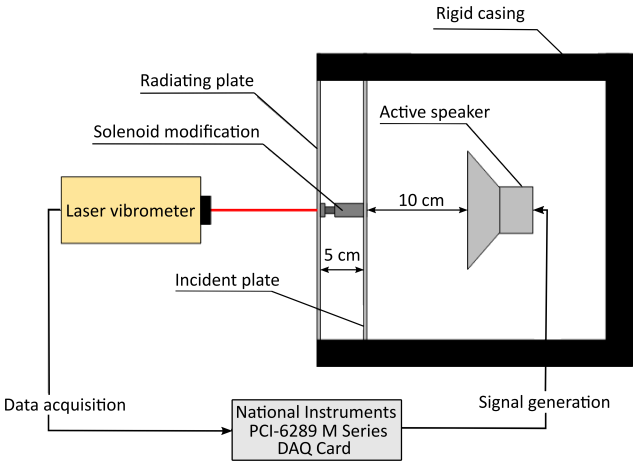

Fig. 2. Experimental setup.

2.2. Double-panel structure coupling

Between two panels of the front rigid casing wall, a semi-active modification was made. At the centre of the radiating panel, a solenoid core was mounted (Fig. 3).

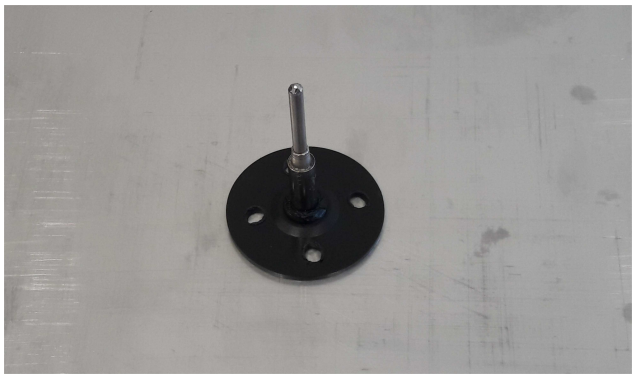

Fig. 3. Solenoid core mounted at the centre of the radiating panel.

At the centre of the incident panel, a solenoid with inductor inside was mounted (Fig. 4). Solenoid was wired to a laboratory power supply. Voltage V from the power supply was either 0 V or 11 V. If V was 0 V, the solenoid core was not held in solenoid inductor mounted on the incident panel, and a possible influence of concentrated mass (solenoid core with plastic wheel used for mounting) was considered only (such case is referred to as case C_{OFF} below). Mass of the solenoid core with plastic wheel used for mounting was measured as $M = 9$ g. If voltage was 11 V, the solenoid core was held in solenoid inductor mounted on the incident panel, hence the radiating panel centre was coupled with the incident panel centre (such case is referred to as case C_{ON} below). It was expected that coupling panels may influence vibroacoustical properties of the radiating panel, and an experiment was performed to analyze such phenomenon.

Fig. 4. Solenoid with inductor mounted at the centre of the incident panel.

2.3. The experiment

Vibrations were measured two times using the laser vibrometer Polytec PDV-100 in each of 49 points of the marked grid on the radiating panel. First measurement in each point was made when voltage was 0 V, and the solenoid core was not held in solenoid inductor mounted on the incident panel. Second measurement in each point was made when voltage was 11 V and the panels were coupled.

The grid dimensions (7×7) are justified experimentally and limited due to technical aspects of the system. As the temperature of the actuator (solenoid) mounted between the plates increases quickly if the current is applied, the undesired local change of structure temperature is observed after specific amount of time. Hence, resonances may be shifted, as panel response varies depending on temperature changes (Mazur, Pawełczyk, 2011). Such phenomenon may influence the results and make them uncredible. As the measurement system allows to measure plate's vibration in one point at once, the total amount of time needed to perform the experiment increases, hence the risk of undesirable structure temperature change increases along with grid dimensions. Grid dimensions are the odd numbers, because maxima and minima of the mode-shapes (up to mode (3,3)) may occur approximately in the points locations.

3. Modeling and simulation

Modeling of double-panel structures is a challenging issue itself, for instance in aerospace sciences (Pietrzko, Mao, 2008). Adding any kind of coupling between panels may increase complexity of calculations. If a model is complex or a broad frequency range is considered, achieving sufficient modeling accuracy and reasonable computation time may be challenging (Klanner, Ellermann, 2018).

In this paper a structure consisting of double panels is considered. Between them, a solenoid is placed, which, if suffiently powered, clamps the panel at its location. Complete mathematical modelling of the structure requires taking into account sophisticated phenomena including fluid-structure interaction and is outside the scope of this paper. It is going to be the subject of another publication. The following experiments show how the response of the structure is changed as compared to the single panel, and demonstrate the potential of this method in noise reduction, particularly if more clamping points are applied. In the following section, basics of single panel vibration analysis are provided to give an overview of issues related to modeling panels, such as influence of additional elements attached to a panel, method accuracy, and modeling assumptions.

In this experiment, it is assumed that rigid casing double-panel walls are built of isotropic steel panels. As steel panels are concerned, it is assumed that Young modulus $E = 200$ GPa, Poisson's ratio $\nu = 0.3$, and panel density $\rho = 7850$ kg/m^3. The radiating panel dimensions are $a \times b \times h = 0.42 \times 0.42 \times 0.0006$ m. Panel

flexural rigidly D is described by the Eq. (1) (Mao, Pietrzko, 2013):

$$D = \frac{Eh^3}{12(1-\nu^2)}, \tag{1}$$

where h is thickness of the panel.

3.1. Free vibrations of a panel

Vibrations of an isotropic panel subjected to lateral static loading $q(x,y)$ may be described by the Kirchhoff-Love model (Timoshenko, Woinowski-Krieger, 1959):

$$D\left(\frac{\partial^4 W(x,y)}{\partial x^4} + 2\frac{\partial^4 W(x,y)}{\partial x^2 \partial y^2} + \frac{\partial^4 W(x,y)}{\partial y^4}\right) = q(x,y), \tag{2}$$

where $W(x,y)$ is an amplitude of the panel lateral displacement.

In case of free vibrations of a panel, it is assumed that lateral loading is replaced by an inertial force (Eq. (3)) (Gorman, 1982):

$$D\left(\frac{\partial^4 W(x,y,t)}{\partial x^4} + 2\frac{\partial^4 W(x,y,t)}{\partial x^2 \partial y^2} + \frac{\partial^4 W(x,y,t)}{\partial y^4}\right) + \rho\frac{\partial^2 W(x,y,t)}{\partial t^2} = 0, \tag{3}$$

where $W(x,y,t)$, referred to as W below, is a function of the space coordinates x, y and time t.

All four edges of each casing panel are connected to a cubic ridig frame by screws and additionally clamped by another square frame, hence fully clamped boundary conditions can be assumed for each panel (Dalaei, Kerr, 1996):

$$\begin{aligned} &W = 0, \quad \frac{\partial W}{\partial x} = 0 \quad \text{at } x = 0 \vee x = a \text{ for } 0 \le y \le b, \\ &W = 0, \quad \frac{\partial W}{\partial y} = 0 \quad \text{at } y = 0 \vee y = b \text{ for } 0 \le x \le a. \end{aligned} \tag{4}$$

Natural frequencies of a square, isotropic, steel panel with fully clamped boundary conditions were calculated based on method proposed in (Mao, Pietrzko, 2013). Values are presented in Table 1.

Table 1. Natural frequencies f_{mn} [Hz] for $m,n = 1,2,3$, calculated using method described in (Mao, Pietrzko, 2013).

m/n	1	2	3
1	29.86	60.97	109.55
2	60.97	90.01	137.2
3	109.55	137.2	182.66

For a comparison, natural frequencies of a panel considered in this paper were also calculated using FreeFem++ (Table 2), which is an open source software designed for solving partial differential equations using the Finite Element Method (FEM). Both methods give similar results. Modes (m,n) and (n,m) for particular m and n in Table 2 are not equal due to assumed modeling accuracy.

Table 2. Natural frequencies f_{mn} [Hz] for $m,n = 1,2,3$, calculated using partial differential equations solver.

m/n	1	2	3
1	29.95	60.73	108.49
2	61.08	89.67	136
3	109.48	136.5	181.28

3.2. Vibrations of a panel loaded with a concentrated mass

To determine the influence of additional element attached to single panel as a concentrated mass, a short analysis is provided below. However such modeling assumptions can not be applied to a double-panel structure, as the solenoid is fastened between two panels, constituting additional point of support, this subsection aims to highlight a general impact of additional elements on vibroacoustics of the panels.

If only single panel would be considered, a solenoid core would be modelled as a concentrated mass located at its centre. One of the approaches for modeling panels carrying a concentrated point mass M located at $(k,\ h)$ employs Rayleigh metod for its simplicity. In such approach, natural frequencies f_{mn} of a panel may be calculated by Eq. (5) (Chai, 1993):

$$f_{mn} = \frac{1}{2\pi}\sqrt{\frac{D_{mn}}{T_{mn}}} \quad [\text{Hz}]. \tag{5}$$

For a panel with all edges fully clamped, D_{mn} and T_{mn} may be calculated from the following equations (Chai, 1993):

- for $m = 1$ and $n = 1$:

$$D_{mn} = \frac{\pi^4 D}{4a^3b^3}(3b^4 + 3a^4 + 2a^2b^2), \tag{6}$$

$$T_{mn} = \frac{9ab\gamma}{64} + M\sin^4\left(\frac{\pi k}{a}\right)\sin^4\left(\frac{\pi h}{b}\right); \tag{7}$$

- for $m = 1$ and $n = 2,3,4,...$:

$$D_{mn} = \frac{\pi^4 D}{32a^3b^3}[16b^4 + 3a^4(1 + 6n^2 + n^4) + 8a^2b^2(1 + n^2)], \tag{8}$$

$$T_{mn} = \frac{3ab\gamma}{32} + M\sin^4\left(\frac{\pi k}{a}\right)\sin^2\left(\frac{n\pi h}{b}\right)\sin^4\left(\frac{\pi h}{b}\right); \tag{9}$$

• for $m = 2, 3, 4, \ldots$ and $n = 1$:

$$D_{mn} = \frac{\pi^4 D}{32a^3b^3}[3b^4(1+6m^2+m^4)+16a^4 + 8a^2b^2(1+m^2)], \quad (10)$$

$$T_{mn} = \frac{3ab\gamma}{32} + M\sin^2\left(\frac{\pi k}{a}\right)\sin^2\left(\frac{m\pi k}{a}\right)\sin^4\left(\frac{\pi h}{b}\right); \quad (11)$$

• for $m = 2, 3, 4, \ldots$ and $n = 2, 3, 4, \ldots$:

$$D_{mn} = \frac{\pi^4 D}{16a^3b^3}[b^4(1+6m^2+m^4)+a^4(1+6n^2+n^4)+ + 2a^2b^2(1+m^2)(1+n^2)], \quad (12)$$

$$T_{mn} = \frac{ab\gamma}{16} + M\sin^2\left(\frac{\pi k}{a}\right)\sin^2\left(\frac{m\pi k}{a}\right) \cdot \sin^2\left(\frac{\pi h}{b}\right)\sin^2\left(\frac{n\pi h}{b}\right), \quad (13)$$

where γ is a mass of the panel per unit area. In the case simulated in this paper, concentrated mass (solenoid core with mounting wheel) $M = 9$ g is located at the centre of the radiating panel, i.e. $k = 0.5a$ and $h = 0.5b$. For an isotropic steel panel examined in this research, considering $m = 1, 2, 3$ and $n = 1, 2, 3$, natural frequencies calculated from Eqs (6)–(13) are presented in Table 3.

Table 3. Natural frequencies f_{mn} [Hz] for $m, n = 1, 2, 3$, $M = 9$ g, calculated using method described in (Chai, 1993).

m/n	1	2	3
1	29.66	63.04	100.15
2	63.04	93.76	135.83
3	100.15	135.83	163.68

The same approach can be employed to calculate free vibrations of a panel without a concentrated mass ($M = 0$ g) (Table 4). The results differ from those obtained in Tables 1 and 2 because of lower method accuracy. However, each of the presented methods may be employed to calculate approximate natural frequencies of a single panel.

Table 4. Natural frequencies f_{mn} [Hz] for $m, n = 1, 2, 3$, $M = 0$ g, calculated using method described in (Chai, 1993).

m/n	1	2	3
1	30.78	63.04	105.78
2	63.04	93.76	135.83
3	105.78	135.83	177.3

Comparison of Tables 3 and 4 implies that a concentrated mass located at the centre of the panel lowers natural frequencies f_{11}, f_{13}, f_{31}, and f_{33}, while frequencies f_{12}, f_{21}, f_{22}, f_{23}, and f_{32} remain unchanged. Values f_{mn} and f_{nm} are equal for each $m \neq n$. Such results are expected in case of a square isotropic panel and confirm correctness of used algorithms. Based on simplified analysis, it is possible that usage of solenoid in proposed double-panel structure modification may cause a decrease of specific resonant frequencies.

4. The experiment results

Figure 5 presents resonant frequencies in the central point of the radiating panel obtained from an experiment, up to 500 Hz. Red line in Fig. 5 corresponds to case of unpowered solenoid, and blue line corresponds to case of activated coupling between panels. Modes f_{mn} and f_{nm} for $m \neq n$ were not distinguished because of square dimensions of the panel. Modes higher than (3,3) were difficult to analyze because of their complicated shape in comparison to grid dimensions.

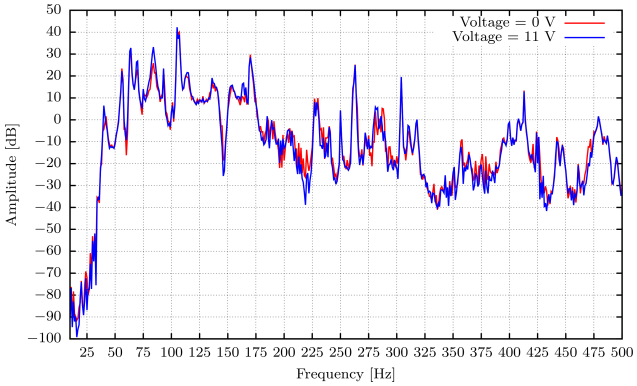

Fig. 5. Comparison of magnitude spectra obtained at voltage $V = 0$ V and 11 V, in the central point of the radiating plate.

Resonant frequencies from Table 3 (f_{22} and f_{33}) are observed in Fig. 5 at about 93 Hz and 163 Hz, respectively. Peak at about 30 Hz (f_{11}) is also observed, however its amplitude is low. Presence of peaks at expected frequencies suggests that there may be similarities between modes (1,1), (2,2) and (3,3) in case of single panel and double-panel structure.

Other resonant frequencies observed in the graph were omitted in the analysis because shapes of plate vibration obtained at them were irregular and hard to analyze. The idea was to observe modeshapes and resonant frequencies of modes (1,1), (2,2) and (3,3), and to compare them to simulation results, as these modes may be observed both in case of single or double panel. As grid dimensions are the odd numbers (7×7), the antinodes of the modeshapes (1,1), (2,2) and (3,3) were supposed to occur approximately in the points locations.

Modeshape obtained at the frequency f_{11} is presented in Figs. 6b (case C_{OFF}) and 6c (case C_{ON}), and compared to modeshape of simulated unloaded iso-

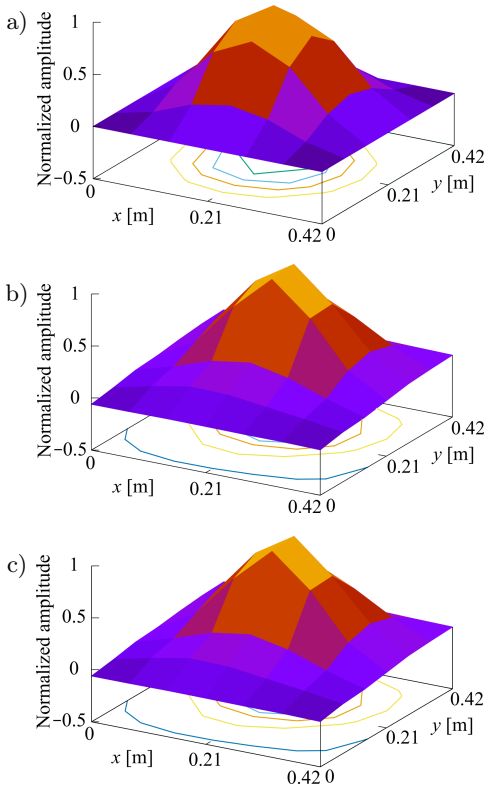

Fig. 6. Comparison of modeshapes at f_{11}: a) simulated unloaded isotropic square panel, b) experimentally measured modeshape at the voltage 0 V, c) experimentally measured modeshape at the voltage 11 V.

tropic square panel (Fig. 6a). Figure 6b corresponds to case of unpowered solenoid. Figure 6c presents modeshape in case of voltage V = 11 V applied to the solenoid. Modeshapes are similar to each other. Surface-averaged vibration amplitude for the whole radiating panel expressed in dB is lower in case C_{ON} (−24 dB) than in case C_{OFF} (−23.07 dB), however such difference is negligible.

In case of resonant frequency f_{22} (93 Hz), applying voltage 11 V to solenoid causes an increase of surface-averaged vibration amplitude ($\overline{A}$) for the whole radiating panel, expressed in dB. In case C_{ON}, $\overline{A}$ equals 10.17 dB, while in case C_{OFF} it is 9.92 dB. A comparison of modeshapes similar to Fig. 6 is presented in Fig. 7.

Similar effect was observed at the frequency f_{33}, where applying voltage 11 V to solenoid caused an increase of surface-averaged vibration amplitude ($\overline{A}$) for the whole radiating panel, from 4.56 dB to 7.07 dB. A comparison of modeshapes similar to Figs 6 and 7 is presented in Fig. 8. As panels coupling is applied once at the centres of them, reduction of vibrations is observed only at mode (1,1). Probably, applying more couplings may provide better results, especially if couplings would be set in minima and maxima of specific modes.

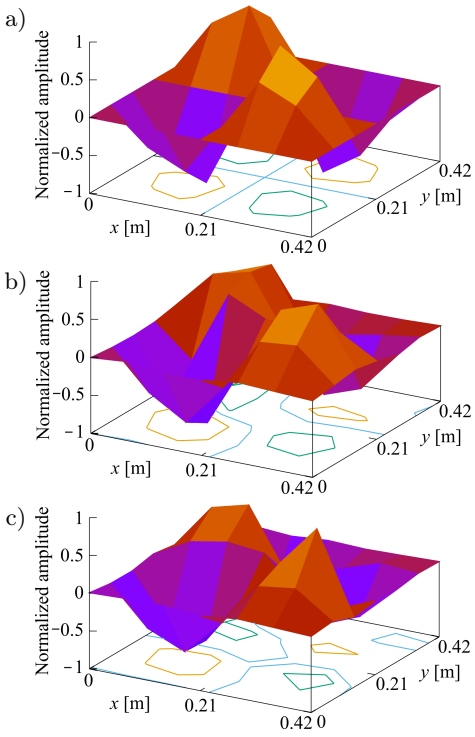

Fig. 7. Comparison of modeshapes at f_{22}: a) simulated unloaded isotropic square panel, b) experimentally measured modeshape at the voltage 0 V, c) experimentally measured modeshape at the voltage 11 V.

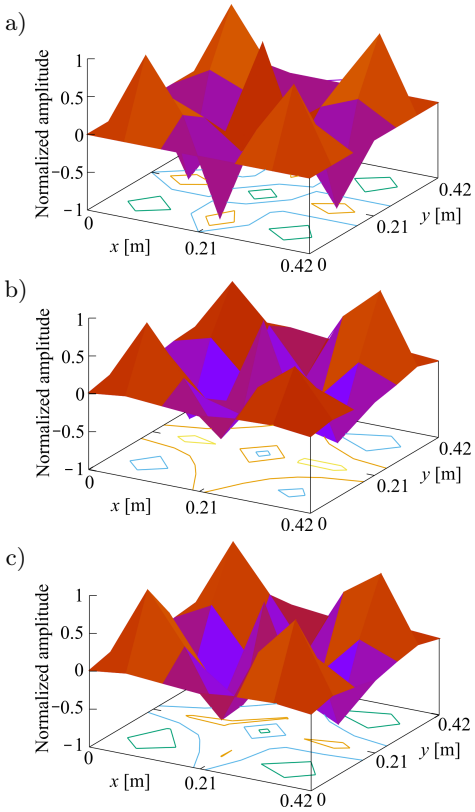

Fig. 8. Comparison of modeshapes at f_{33}: a) simulated unloaded isotropic square panel, b) experimentally measured modeshape at the voltage 0 V, c) experimentally measured modeshape at the voltage 11 V.

Figures 6–8 confirm correctness of performed experiment, and indicate significant influence of solenoid core mass on resonances even if the solenoid is unpowered. If voltage 11 V is applied to the solenoid, mode-shapes do not change significantly – their maxima and minima remain in the same locations. However, amplitude of vibrations may increase or decrease, depending on the frequency.

To compare panel vibrations at the frequencies up to 500 Hz in both cases, i.e. C_{OFF} and C_{ON}, surface-averaged vibration amplitude for the whole radiating panel (referred to as $\overline{A}$) was calculated and expressed in dB. Results are presented in Fig. 9. Decrease of such value may indicate general reduction of panel vibrations. Change of vibrations was not compared in particular points, because high vibration amplitude may be transferred to another area of the panel. In Fig. 9a, comparison of $\overline{A}$ calculated for both cases is presented. The analysis took into account two biggest differences (Fig. 9b) between them. At the frequencies up to 500 Hz they are observed at the frequencies 25 Hz and 427 Hz.

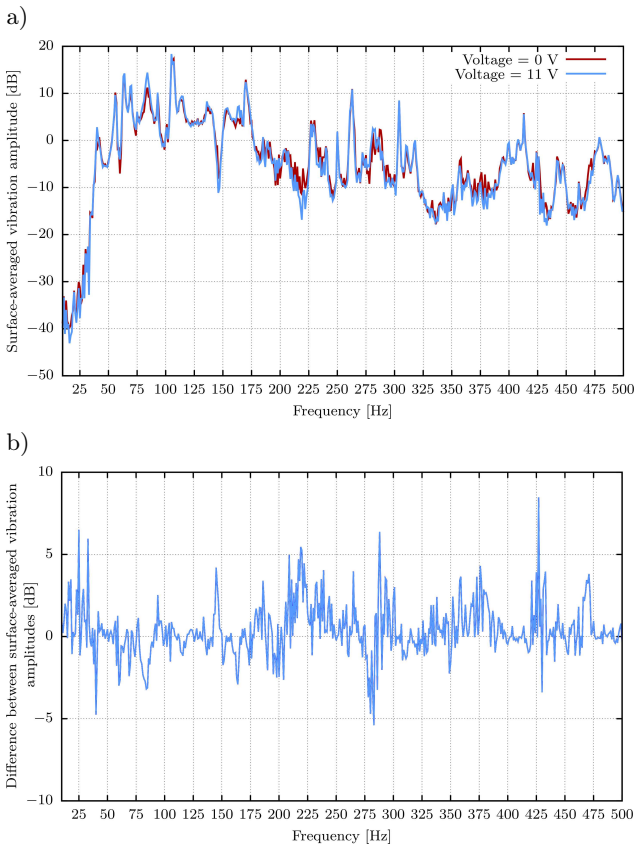

Fig. 9. a) Comparison of surface-averaged vibration amplitude for the whole radiating panel, calculated for cases C_{OFF} and C_{ON}; b) difference between surface-averaged vibration amplitudes for the whole radiating panel, calculated for cases C_{OFF} and C_{ON}.

Shape of panel vibrations at the frequency 25 Hz is presented in Fig. 10. If panels are not coupled

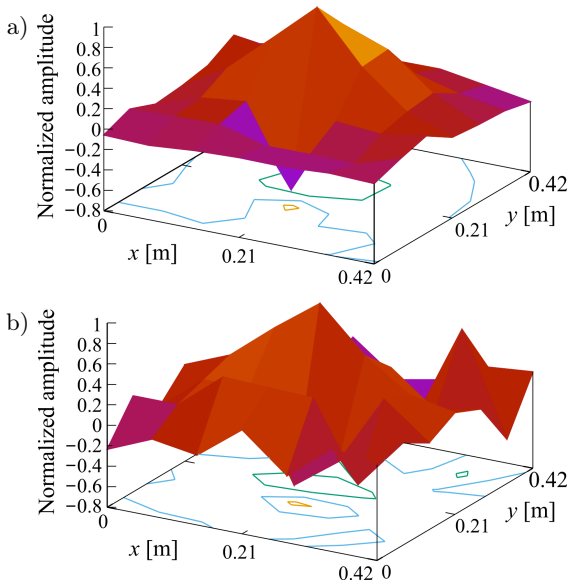

Fig. 10. Normalized amplitudes of panel vibrations on 7×7 grid at 25 Hz: a) case C_{OFF}, b) case C_{ON}.

(case C_{OFF}, Fig. 10a), it significantly differs from the shape of panel vibrations observed in case of coupled panels (C_{ON}, Fig. 10b). Activating coupling between panels causes a significant decrease of $\overline{A}$, from −31.24 dB to −37.74 dB.

In Fig. 11, the shape of panel vibrations at the frequency 427 Hz is presented. In case of unpowered solenoid (C_{OFF}, Fig. 11a), it is significantly different than the shape of panel vibrations calculated for coupled panels (C_{ON}, Fig. 11b), however, comparison of normalized panel shapes does not provide important information about surface-averaged vibration reduction. Activating coupling between panels causes a de-

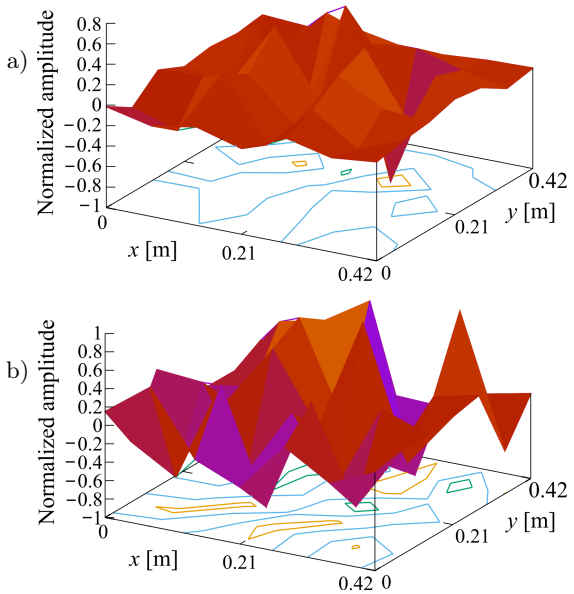

Fig. 11. Normalized amplitudes of panel vibrations on 7×7 grid at 427 Hz: a) case C_{OFF}, b) case C_{ON}.

crease of $\overline{A}$, from −7.28 dB to −15.76 dB, which is a result even better than in case of frequency 25 Hz.

5. Summary and conclusions

Analysis provided in Sec. 4 shows that results obtained experimentally are consistent with simulation output, however only in case of modes (1,1), (2,2) and (3,3). There are many other resonant frequencies, which have to be analyzed in comparison to the double-panel structure model. Such model is out of scope of this paper, but in future publications it has to be taken into account, as many complicated phenomena occur in case of double-panel structures. Modeling approach presented in this paper allowed only to calculate approximate values of expected natural frequencies of the radiating panel with solenoid core mounted at its centre for modes (1,1), (2,2) and (3,3).

The aim of semi-active modification of double-panel structure described in this paper was to notice its influence on vibroacoustical properties of the radiating panel. At one of resonant frequencies, f_{11} (30 Hz), applying voltage to solenoid and coupling panels reduced surface-averaged amplitude over 49 grid points. However, in case of f_{22} (93 Hz) and f_{33} (163 Hz), surface-averaged amplitude over 49 grid points increased. The amplitude was lowered significantly only at the panel centre, where the coupling was applied. Such effect may be caused by limited vibration of the radiating panel's centre if the panels were coupled. The panels coupling is applied only once, at the centres of panels. Slight reduction of vibrations is observed at mode (1,1). Applying more panels couplings at different coordinates may provide reduction of vibrations also at higher modes, especially if couplings would be applied in the antinodes of such modes.

Beyond the resonant frequencies, interesting effects were observed at 25 Hz and 427 Hz, where applied coupling of the panels caused the two most significant changes in shape of panels vibrations, and reduced amplitude of vibrations in general.

Acknowledgments

The research reported in this paper has been supported by the National Science Centre, Poland, decision no. DEC-2017/25/B/ST7/02236.

References

1. Alimohammadi I., Ebrahimi H. (2017), *Comparison between effects of low and high frequency noise on mental performance*, Applied Acoustics, **126**: 131–135, doi: 10.1016/j.apacoust.2017.05.021.
2. Bao C., Pan J. (1997), *Experimental study of different approaches for active control of sound transmission through double walls*, The Journal of the Acoustical Society of America, **102**(3): 1664–1670, doi: 10.1121/1.420105.
3. Chai G.B. (1993), *Free vibration of rectangular isotropic plates with and without a concentrated mass*, Computers & Structures, **48**(3): 529–532, doi: 10.1016/0045-7949(93)90331-7.
4. Chrapońska A., Wrona S., Rzepecki J., Mazur K., Pawełczyk M. (2019), *Active structural acoustic control of an active casing placed in a corner*, Applied Sciences, **9**(6): 1059, doi: 10.3390/app9061059.
5. Dalaei M., Kerr A.D. (1996), *Natural vibration analysis of clamped rectangular orthotropic plates*, Journal of Sound and Vibration, **189**(3): 400, doi: 10.1006/jsvi.1996.0026.
6. Elliott S.J. (2001), *Signal processing for active control*, Academic Press, London.
7. Gorman D.J. (1982), *Free vibration analysis of rectangular plates*, Elsevier, New York.
8. Kim H.S., Kim S.R., Lee S.H., Seo Y.H, Ma P.S. (2016), *Sound transmission loss of double plates with an air cavity between them in a rigid duct*, Journal of the Acoustical Society of America, **139**(5): 2324–2333, doi: 10.1121/1.4946987.
9. Klanner M., Ellermann K. (2018), *Improvement of the wave based method for thick plate vibrations*, The International Journal of Acoustics and Vibration, **23**(4): 492–505, doi: 10.20855/ijav.2018.23.41222.
10. Leniowska L., Sierżęga M. (2019), *Vibration control of a circular plate using parametric controller with phase shift adjustment*, Mechatronics, **58**: 39–46, doi: 10.1016/j.mechatronics.2019.01.003.
11. Ma X., Chen K., Ding S., Yu H. (2016), *Physical mechanisms of active control of sound transmission through rib stiffened double-panel structure*, Journal of Sound and Vibration, **371**: 2–18, doi: 10.1016/j.jsv.2016.02.009.
12. Mao Q., Pietrzko S.J. (2013), *Control of noise and structural vibration. A Matlab – based approach*, Springer, London.
13. Mazur K., Pawełczyk M. (2011), *Active noise-vibration control using the filteredreference LMS algorithm with compensation of vibrating plate temperature variation*, Archives of Acoustics, **36**(1): 65–76.
14. Morzyński L., Szczepański G. (2018), *Double panel structure for active control of noise transmission*, Archives of Acoustics, **43**(4): 689–696, doi: 10.24425/aoa.2018.125162.
15. Oliazadeh P., Farshidianfar A., Crocker M. (2019), *Study of sound transmission through single- and double-walled plates with absorbing material: Experimental and analytical investigation*, Applied Acoustics, **145**: 7–24, doi: 10.1016/j.apacoust.2018.09.014.
16. Pietrzko S.J., Mao Q. (2008), *New results in active and passive control of sound transmission through double wall structures*, Aerospace Science and Technology, **12**(1): 42–53, doi: 10.1016/J.AST.2007.10.006.

17. Rzepecki J., Chrapońska A., Mazur K., Wrona S., Pawełczyk M. (2019), *Semiactive reduction of device casing vibration using a set of piezoelectric elements*, Manuscript submitted to 14th Conference on Active Noise and Vibration Control Methods 2019, Krakow-Wieliczka, Poland.
18. Sibielak M., Rączka W., Konieczny J., Kowal J. (2015), *Optimal control based on a modified quadratic performance index for systems disturbed by sinusoidal signals*, Mechanical Systems and Signal Processing, **64–65**: 498–519, doi: 10.1016/j.ymssp.2015.03.031.
19. Timoshenko S., Woinowski-Krieger W. (1959), *Theory of plates and shells*, 2nd ed., McGraw-Hill, New York.
20. Wrona S., Pawełczyk M. (2018), *Feedforward control of double-panel casing for active reduction of device noise*, Journal of Low Frequency Noise, Vibration and Active Control, 3–5, doi: 10.1177/1461348418811429.